Finite element method analysis of transverse crack onset strain for cross-ply CFRP laminates with thin and thick ply thickness

The finite element method (FEM) analysis with ABAQUS/CAE using Drucker-Prager elastoplastic damage model in the matrix, cohesive zone model in fiber-matrix and 0°–90° layer interfaces were performed.

Figure S1 shows the (a) reference image, (b) cross-ply with thin ply thickness, and (c) cross-ply with thick ply thickness models.

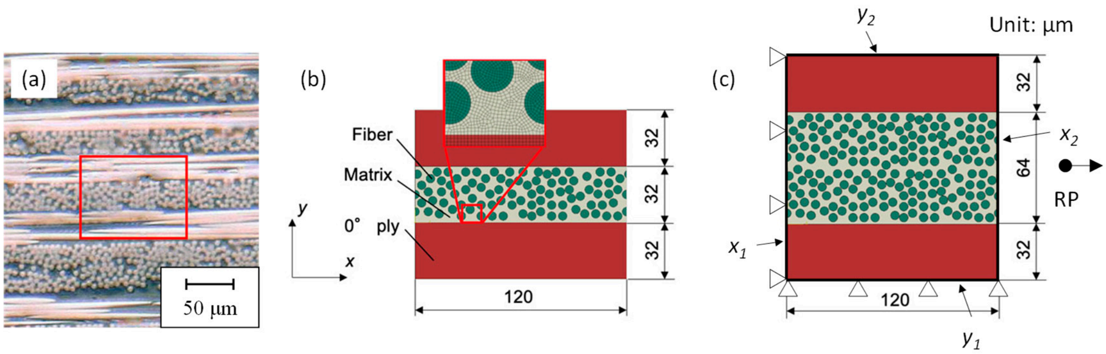

Figure S1 (a) reference image, (b) representative volume element (RVE) of cross-ply with thin ply thickness, and (c) RVE of cross-ply with thick ply thickness models.

The red colors showed the 0° ply. The fiber distributions in 90° ply were decided on the reference image. The boundary conditions are also shown in the figure. The lines x_1 and y_1 were pinned on the x and y-axis, respectively. Lines x_2 and y_2 have the same x and y displacements. The reference point was set to apply the 1.2 μm (a nominal strain of 1 %) of displacement. The analysis model was a two-dimensional plain strain model formed by isoparametric quadrilateral elements. The number of elements and nodes were (a) 83008, 91895 and (b) 117701, 134048, respectively.

The material properties are presented in **Table S1**. The modulus and Poisson's ratio of CFRP were obtained from the tensile tests for unidirectional CFRP specimens with 0°, 45°, and 90° fiber orientations (specimen dimensions, testing machine, and testing conditions) the same). The matrix was modeled with elastoplastic damage material, and the plastic behavior of the matrix was used for the hyperbolic-type Drucker-Prager model. The material properties of the matrix were decided based on the literature [S1]. The cohesive zone models were introduced in the fiber/matrix and layer (0°/90°) interfaces. The damage initiation and propagation criteria were applied with the ellipse rule of traction and the *energy release rate B-K criterion*. The material characteristics of the fiber/matrix interface were decided according to the literature [S1].

The material properties of the layer interface were obtained from the double cantilever beam and end-notched flexure tests for unidirectional CFRP specimens with 0° fiber orientation. The specimen dimensions, testing machine, and testing conditions were the same as in the literature [S2].

Table S1 Material properties for FEM analysis.

Fiber	Transverse Young's modulus	17.5 GPa
	Transverse Poisson's ratio	0.46
	Longitudinal shear modulus	15.9 GPa
Matrix	Young's modulus	3.76 GPa
	Poisson's ratio	0.39
	Drucker-Prager Friction angle	35 °
	Drucker-Prager Initial hydrostatic strength	42.16 GPa
	Drucker-Prager Dilatation angle	35 °
	Ductile damage Tensile failure strain	0.008
	Ductile damage Compressive failure strain	0.025
	Ductile damage Hydrostatic failure strain	1.0×10^{-10}
	Ductile damage Fracture toughness	15 J/m^2
CFRP	Longitudinal Young's modulus	152 GPa
	Transverse Young's modulus	8.21 GPa
	Longitudinal Poisson's ratio	0.26
	Transverse Poisson's ratio	0.46
	Longitudinal shear modulus	4.0 GPa
Fiber/matrix interface	Mode I maximum traction	53 MPa
	Mode II&III maximum traction	0.17 MPa
	Mode I fracture toughness	15 J/m^2
	Mode II&III fracture toughness	45 J/m^2
	B-K mode parameter	1.45
0°/90° interface	Mode I maximum traction	71 MPa
	Mode II&III maximum traction	97 MPa
	Mode I fracture toughness	329 J/m^2
	Mode II&III fracture toughness	915 J/m^2
	B-K mode parameter	1.634

The distributions of the in-plane principal plastic strain of cross-ply CFRP laminates with thin and thick ply thickness are compared in **Figure S2**.

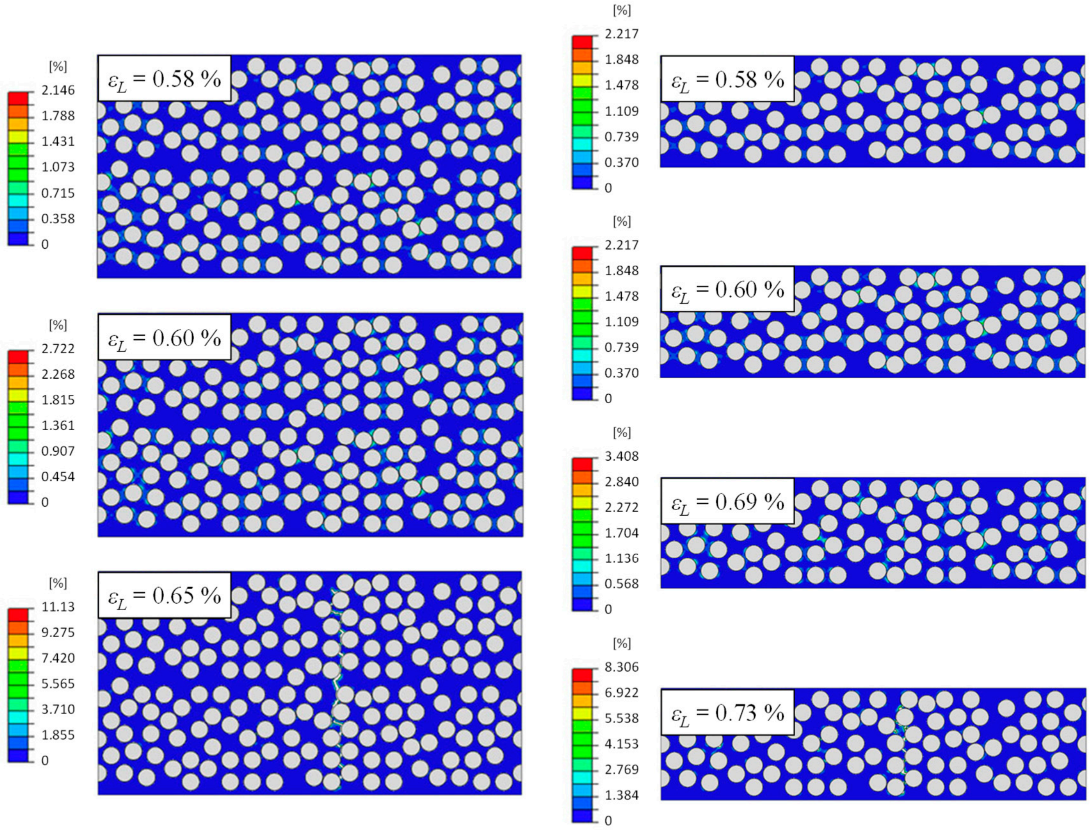

Figure S2 In-plane principal plastic strain distributions of cross-ply CFRP laminates with thin and thick ply thickness.

The plastic strain was concentrated in the fiber aggregation area, and debonding occurred in the fiber/matrix interface. The plastic strain increased near the debonding area, and then the matrix near the debonding area failed. A clear transverse crack was formed. The transverse crack for cross-ply CFRP laminate with thick ply thickness formed in a nominal tensile strain of 0.65%. However, a transverse crack of cross-ply CFRP laminated with thin ply thickness formed at the nominal tensile strain of 0.73%. The transverse crack onset strain of thin-90°-ply was higher than that of thick-90°-ply. Therefore, the tensile strength and failure strain of cross-ply CFRP laminate with thin ply thickness was higher than those of cross-ply with thick ply thickness one. The constraint effects of 0° layers were significant, and the onset of transverse matrix cracking through the thickness of the ply, delamination damage, and fiber breakage was suppressed.

References

S1. Higuchi, R., Aoki, R., Yokozeki, T., Okabe, T. Evaluation of the in-situ damage and strength properties of thin-ply CFRP laminates by micro-scale finite element analysis. Adv Compos 2020, 29, 475–493. https://doi.org/10.1080/09243046.2020.1740867

S2. Naito, K., Nagai, C. Mode-I and mode-II interlaminar fracture properties of high modulus pitch-based carbon fiber rein-forced polymers containing different nanostructures. J Compos Mater 2022, 56, 397–407. https://doi.org/10.1177/00219983211049289